Material Characterization of Polyolefins by Synchrotron X-ray and Neutron Scattering

Sumitomo Chemical Co., Ltd.
Petrochemicals Research Laboratory
Takashi SAKURAI
Yoshinobu NOZUE
Tatsuya KASAHARA*
Noboru YAMAGUCHI

Synchrotron X-ray and neutron scattering are very useful methods to investigate the hierarchical structure and structure-property relationship of polymeric materials at a microscopic level. Our company makes extensive use of quantum beams such as those from synchrotron and neutron sources in cooperation with advanced research facilities for deeply understanding the nature of polymeric materials. In this paper, we introduce state-of-art experimental techniques and industrial applications of advanced quantum beam sources to polyolefin materials as part of our research activities.

This paper is translated from R&D Report, "SUMITOMO KAGAKU", vol. 2007-II.

Introduction

In recent years we see and hear the character "quantum beam." Quantum beam is a general term for high quality beams of particles such as neutrons, photons, electrons, ions, neutrinos supplied by accelerators, nuclear reactors, high output laser devices, etc., and they are used in many fields, such as material science including soft materials, life science and medical treatment. One method for evaluating substances using these quantum beams is the method of analyzing structures on a wide scale from the sub-nanometer level to the micrometer level from the scattering of a quantum beam irradiated to the material. Quantum beams make a large contribution to the elucidation of structural evolution processes and mechanisms for the generation of functions in functional materials and composite materials as a measurement probe for the morphology of substances in special environments and atmospheres, hierarchical aggregate structures, etc. In addition, recent years have shown a trend toward increasing use of quantum beams in industry in the same way as in academic research fields, and this trend is the same in the polymer industry. As a driving force for promoting advanced science and technology and creating new scientific fields, and as a powerful tool for contributing to the development of products in industry, we can expect even more progress in the performance of quantum beams and an increase in opportunities for using them.

At Sumitomo Chemical, we are actively promoting research at facilities outside of the company in areas such as synchrotron radiation and neutrons.[1)–8)] In this paper, we will introduce state-of-art experimental techniques for advanced quantum beams and their applications for research on the structure-property relationships of polyolefin materials through examples of *in-situ* observation techniques of film drawing process and evaluation of molded products using X-ray and neutron scattering.

Research on the Use of Synchrotron Radiation

1. Synchrotron Radiation X-ray Scattering [9)]

When X-rays are incident to a substance, they are scattered by the electrons in the substance, and we can obtain information about the structure of the substance by measuring the scattered x-rays. Most polymers consist of hierarchical structures, such as the crystal lattice, periodic lamellar structures and spherulites shown in **Fig. 1**, on a wide scale from the sub-nanometer level to the micrometer level. It is possible to evaluate the packing and the degree of orientation of crystals using wide-angle X-ray scattering (WAXS), and the sizes and arrangements of lamellar structures (scattering caused by differences in electron density in crystalline parts (Cr) and non-crystalline parts (Am)) using small-angle

* Currently employed by Rabigh Refining & Petrochemical Company.

X-ray scattering (SAXS). Therefore, X-ray scattering is an indispensable method for structural research on polymers, but within this, the quality of the structural information obtained can be dramatically improved by using synchrotron radiation as the source of radiation for the scattering.

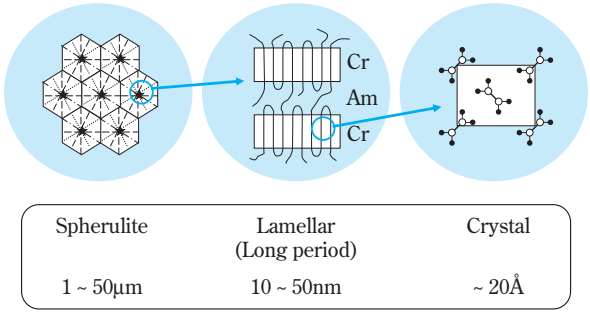

Fig. 1 Hierarchical structure of polyolefin material

Synchrotron radiation consists of electromagnetic waves generated when electrons moving at speeds near the speed of light in an accelerator are accelerated by electromagnets and their direction of travel is changed. **Fig. 2** shows the principle schematically.

The characteristics of synchrotron radiation that can be cited include 1) it is extremely bright; 2) it has a continuous spectrum over a wide range of wavelengths from the infrared to X-rays; 3) an X-ray beam with high directivity is obtained; and 4) the beam is linearly or circularly polarized. Brightness is the number of X-ray photons present per unit time, unit surface area, unit solid angle and specific wavelength range ($d\lambda/\lambda$), and the brightness of synchrotron radiation reaches 100 million times that from a normal X-ray generator.

The characteristic of synchrotron radiation being ultra-bright means that structural information that required several hours for measurement using normal X-ray generators can be acquired in times in the order of milliseconds. This is a sufficient time resolution to trace the changes in nano-structures during film drawing behavior and melt-crystallization processes under an external force. In addition, it is possible to achieve the generation of an ultra-bright highly directed X-ray micro-beam by using a condensing optical system such as a total reflection mirror or a Fresnel zone plate. Moreover, the characteristic of having high directivity means that the scattered x-rays are effective for measuring smaller angles of scattering with high angular resolution, and they exhibit their strength even in the evaluation of the extreme surfaces (several nm) of thin films.

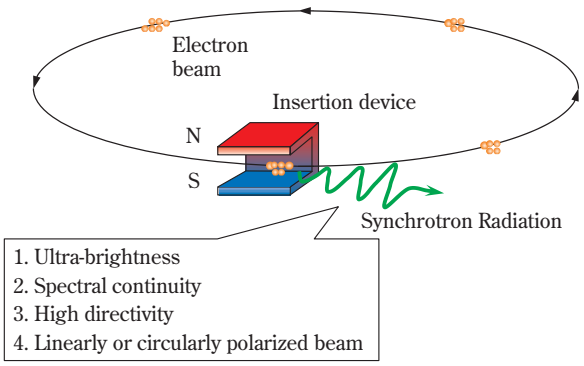

Fig. 2 Generation of Synchrotron Radiation

X-ray scattering measurements using synchrotron radiation can basically have the same setup as measurements by conventional X-ray generators, and may take the form of optical systems where from the light source there is a sequence of a slit system, a sample part and a detector in that order. In addition, the performance of the detector is as important as the light source, and a pulse measurement type or integration type is selected according to the purpose of the measurements. In recent years, accompanied by the development of two-dimensional detectors of which CCD X-ray detectors[10] capable of time-resolved measurements are representative, and also due to advances in experimental technology, it has become possible to carry out simultaneous two-dimensional WAXS/SAXS measurements that simultaneously trace anisotropic nano and sub-nano structural changes under an external field such as shear on millisecond order.

2. *In-situ* Observations of Film Drawing Behavior

(1) *In-situ* Observations of Film Uniaxial Drawing[3), 4)]

In-situ observations of melt crystallization processes and deformation behavior of polymer are a representative type of research that uses synchrotron radiation. It is used in *in-situ* observation of the crystallization process in shear flow, dynamic analysis of phase transition phenomena in multi-component systems and *in-situ* observation of deformation behavior in films, fiber and rubber. Among these, there are examples of research where melt spinning machines and injection molding machines are actually brought into the radiation facilities and *in-situ* observations of the crystallization process and phase separation behavior in the reactive polymer processing.

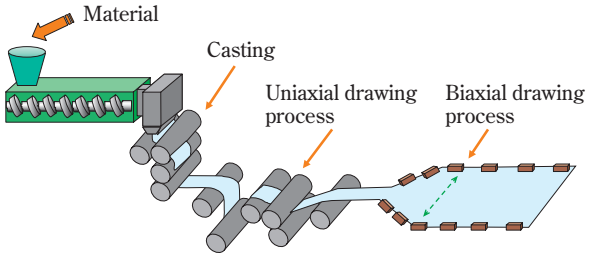

Fig. 3 Schematic illustration of sequentially biaxial drawing process

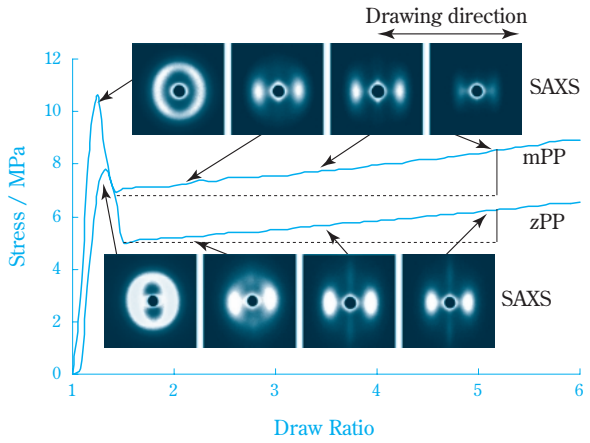

Fig. 4 Stress-strain curves and corresponding time-resolved 2D SAXS patterns

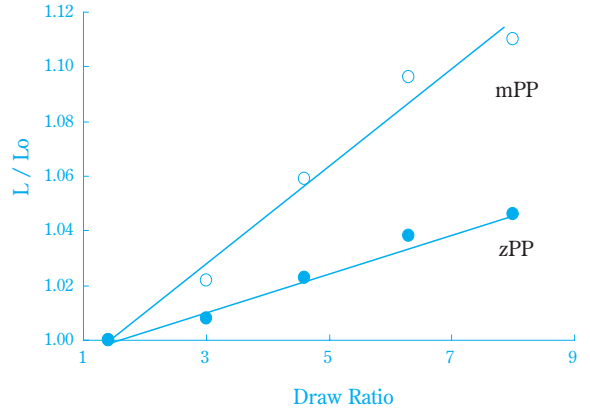

Fig. 5 Changes of long period as a function of DR ; L/Lo is normalized value by dividing long period at each DR by that obtained at the point just beyond necking

We will describe the example of sequential biaxial drawing process, which is a drawing system for polypropylene, shown in **Fig. 3**. Multiple rollers are used for the uni-axial drawing processes, and the polypropylene is drawn by the difference in the speed of rotation of these rollers. The deformation mechanism is necking. In such cases, we can approximately understand the phenomena occurring during the drawing process by investigating the deformation behavior through tensile tests.

Fig. 4 and **Fig. 5** show examples of comparative studies of hot drawing behavior (drawing temperature of 120°C and drawing rate of 10% strain/sec.) for a Zieglar-Natta catalyst polypropylene (zPP) and a metallocene catalyst polypropylene (mPP). *In-situ* observations of hot drawing behavior were carried out at the small angle X-ray scattering station (BL-15A) at the High Energy Accelerator Research Organization. In addition, the basic characteristics of the samples used in the experiments are summarized in **Table 1**.

As is shown in Fig. 4, the yield stress (DR = 1.2) and changes in drawing stress after necking (DR = 1.5 – 6.0) differ according to the sample, and the fact that the differences in the drawing stress are differences in the higher order structural changes in the polypropylene are reflected in the SAXS images.

With mPP, only a spot shaped SAXS image was observed in the drawing region after necking in the direction of drawing, but with zPP, a streak-like SAXS image was observed in the direction orthogonal to the direction of drawing in addition to the spot shaped SAXS image. The spot shaped SAXS images are scattering caused by the interval (long period) of lamellar structures arranged in the direction of drawing, and they are shown by the comparisons of the draw ratio dependency of the changes in the long period in Fig. 5. It can be seen that mPP has greater long period changes than zPP.

As mentioned above, synchrotron radiation is a powerful tool for investigating the correlations between structures and physical properties, and we can imagine

Table 1 Characteristics of iPP samples

Sample	*Mw*	*Mw/Mn*	CXS[a] (wt%)	[mmmm][b]	[η]	Tm (°C)	Density (g/cm^3)
zPP	435,000	5.1	4.0	0.91	2.1	160.9	0.901
mPP	364,000	1.9	0.1	>0.99	2.2	160.1	0.905

[a]Fraction soluble in *p*-xylene at 20°C

[b]Isotactic pentad fraction determined by ^{13}C NMR

the mechanisms generating drawing stress with connections to structural changes in the nano scale level. It is assumed that the higher order structures of polypropylene that has a narrow distribution of molecular weight like mPP are comparatively uniform. While the lamellar structures contribute cooperatively to the deformation during drawing and require a large drawing stress, polypropylene that has a broader distribution of molecular weight like zPP has a wider distribution of lamellar structures such that there are lamellar structures from ones that do not contribute very much to deformation to those that are easily deformed. For drawing, it can be seen that some of the lamellar structures occur the plastic deformation to the extent that regularity is lost.

(2) *In-situ* Observations of Film Biaxial Drawing

In a tentering sequential biaxial drawing process for polypropylene, the film, which is the product, is manufactured as is shown in Fig. 3 by vertical uniaxial drawing and horizontal biaxial drawing. Therefore, to investigate the hot deformation behavior in the horizontal drawing which is a continuous process following the vertical drawing, we developed a prototype of a small hot biaxial drawing machine[11], and successfully applied to observe the sequential biaxial drawing behavior of polypropylene.

Fig. 6 shows an overview of the machine as well as an example of the SAXS and WAXS images observed in sequential biaxial drawing tests (drawing temperature 160°C, drawing rate 10% strain/sec.). With this machine, there is a mechanism where the upper and lower and left and right pairs of drawing bars move only the same distance in the opposite directions respectively, and drawing operations such as simultaneous biaxial drawing and sequential biaxial drawing can be carried out. In addition, to observe the drawing behavior, we designed the machine so that the X-rays irradiated the center of the sample that was normally in a static state during drawing.

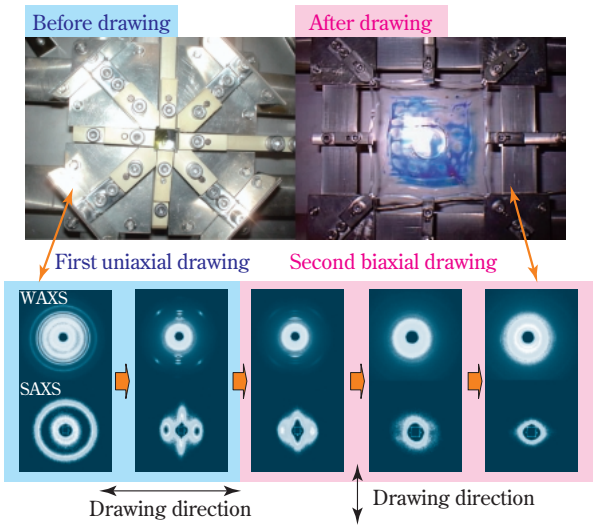

Fig. 6 Newly designed biaxial drawing machine and changes of WAXS and SAXS patterns observed during sequentially biaxial drawing process

The samples used were the zPP described in Table 1, and while the drawing temperature was changed, the same SAXS images were observed in the first uniaxial drawing process compared with those described in the previous section. In addition, the WAXS images showed the c-axis orientation of alpha-typed crystallites to the direction of drawing. In the process where drawing in the orthogonal direction (biaxial drawing) was carried out following uniaxial drawing, the spot shaped SAXS image changed to an arc shape at a comparatively early stage, and while there was a transition to the biaxial drawing direction after cleavage, we obtained very interesting results such as the shape of the streak-like SAXS image gradually changing from a diamond shape to a circular shape. This information about the structural changes at the nano scale is useful information for proposing new designs for poymer materials.

3. Local Structure Analysis Using Microbeam X-Rays[5), 12)]

Microbeam X-rays that have been narrowed down to micron size have applications in evaluating the spatial nonuniformity of nanostructures, such as evaluation of the hierarchical structures in single fibers, human hair and polymer spherulites. To carry out even more detailed examinations on necking deformation, we made a new attempt at *in-situ* observations of hot drawing behavior of polypropylene spherulites. **Fig. 7** shows the layout of the *in-situ* observation tests for drawing behavior using simultaneous microbeam WAXS- SAXS measurements carried out at the beam line (BL40XU) at SPring-8.

In this method, both a system for observing the relationship between the viewpoint of the sample and the irritated spot of the microbeam using a polarized optical microscope (POM) and a tensile testing machine[13] capable of moving the sample position with a precision of 1 μm were used for keeping the relationship between the measured location of the sample and the

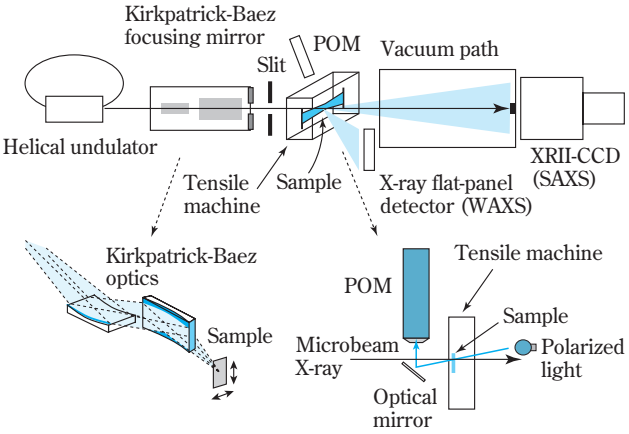

Fig. 7 Experimental setup for in-situ microbeam SAXS-WAXS simultaneous measurement

microbeam position constant during drawing.

Fig. 8 shows representative POM, SAXS and WAXS-data sets of zPP obtained using the *in-situ* observations of the hot drawing behavior. The major feature of this method is being able to evaluate the deformation behavior as well as the spatial distribution of the nanostructures formed in one spherulite. From the SAXS image in the horizontal direction and the WAXS image in the vertical direction on the paper, information regarding the crystallites and long period of the structures which are called the "parent lamellae" that have grown in the radial direction of the spherulite and information regarding the structures called the "daughter lamellae" formed with a different orientation from the parent lamellae can be evaluated from the SAXS image in the vertical direction and the WAXS image in the horizontal direction on the paper. On the other hand, a ring shaped pattern is observed for conventional X-rays. The conventional X-ray beam has a larger beam diameter, so the lamellar structures formed in all directions in many spherulites are observed in the WAXS and SAXS measurements before deformation.

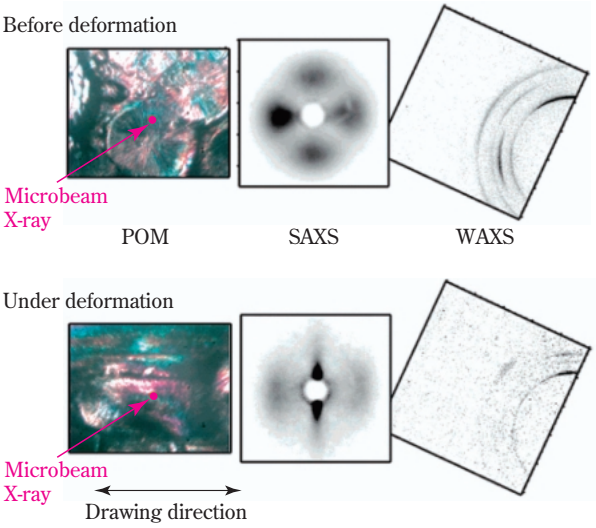

Fig. 8 Representative POM-SAXS-WAXS data sets of zPP observed during hot drawing

Fig. 9 shows an example of analytical results from the changes in long period and full width at half maximum (FWHM) for the SAXS profile in the parent lamellae and daughter lamellae during drawing. It can be seen that the long period and the FWHM for the parent lamellae start changing at an early stage of deformation with small frame numbers. From detailed investigations including these, it is clear that there are at least two steps in the deformation behavior of zPP, that is, 1) deformation of the parent lamellae that are arranged in the direction of drawing at first, and 2) then deformation of the daughter lamellae occurs in the drawing region where the parent lamellae fragmentation occurs. We think that further investigations of lamellar structural deformation behavior in different observation locations will play an important role to clarify the deformation mechanism.

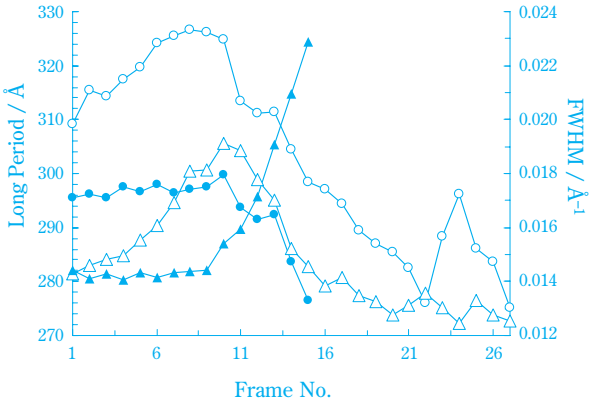

Fig. 9 Changes in long period and FWHM in parent and daughter lamellae obtained from the sector averaged SAXS profiles of zPP ;
○ long periods (parent lamellae),
● long periods (daughter lamellae),
△ FWHM (parent lamellae),
▲ FWHM (daughter lamellae)

Research into the Use of Neutrons

1. Neutron Scattering [14), 15)]

A neutrons is a Fermi particle with a charge of 0, a mass of 1u (u: atomic mass unit = 1.661×10^{-27} kg) and a spin of 1/2. The features are 1) reaching the atomic nucleus without being shielded by electrons that surround the atomic nucleus and being scattered by atom-

ic nuclei because of the charge of 0, as well as 2) being scattered by the magnetic field when the electrons that are around the atomic nucleus make a magnetic field because of a spin of 1/2. **Fig. 10** shows a schematic illustration of these principles. The scattering phenomena due to neutrons is roughly divided into scattering where there is no energy exchange between the substance and the neutrons, which is called elastic scattering, and inelastic scattering which is accompanied by an exchange of energy. Small angle neutron scattering (SANS), which is used in structural research from the nanometer scale to the micron scale, ultra-small angle neutron scattering (U-SANS), neutron reflectometry (NR) which is used for structural evaluation of surface and interface in items such as thin films and multilayered films, are classified into the former elastic scattering phenomena.[16] The latter are mainly applied to dynamic research such as lattice vibration and polymer segment motion, and there are various methods used such as neutron spin echo (NSE) and quasi-elastic neutron scattering (QENS).

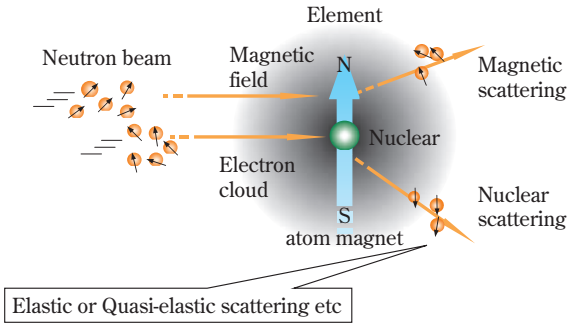

Fig. 10 Schematic illustration of neutron scattering

The neutron is an extremely effective probe for structural research on polymers including soft materials, and scattering methods with neutrons as the source have unique features caused by the scattering origin that is different from optical scattering and X-ray scattering. **Table 2** gives a comparison in the characteristics of SAXS using synchrotron radiation and SANS. The basic principles of the scattering are the same even in cases where neutrons are used, and synchrotron radiation SAXS is superior at various levels of flux (brightness) and resolution. However, as is shown in the comparison in **Table 3**, the scattering length of atomic nuclei for neutrons differs greatly between hydrogen (H) and deuterium (D), and this difference gives a distinct scattering contrast in SANS. Since most soft materials such as polymers contain hydrogen, it is possible to directly examine the conformation of the polymer chains in bulk or solutions and the interaction between different polymer chains by measuring the D-H scattering contrast with SANS by substituting D for H (deuterium labeling) in specific molecules in aggregate polymer systems and using D_2O in solution. In terms of other characteristics, the fact that the energy of SANS is lower than that of SAXS can be cited, and the point that there is little damage to the material with neutron irradiation is a merit for biological materials as well as soft materials.

There are mainly two sources of neutrons;one is stationary neutrons from nuclear fission and chain reaction of ^{235}U fuel from nuclear reactors, and the other is pulse neutrons generated by accelerators, but the main source for SANS is cold neutrons (neutrons with a long wavelength which have been cooled by a coolant such as liquid hydrogen) from nuclear reactors. In SANS experiments, basically there is an optical system with a sequential arrangement of a monochromator that makes the cold neutrons having a wavelength distribution that are emitted from a nuclear reactor the monochromatic wave, a pinhole collimator that limits the direction of travel of the monochromatic neutrons with high precision, a sample part and a detection part with a detector built into a moving vacuum tube. The position of the collimator and thedetector are usually

Table 3 Neutron scattering length of fundamental elements

	H	D	C	N	O
Scattering length/fm	–3.74	6.67	6.65	9.40	5.80

fm = 10^{-15}m

Table 2 Comparison of SAXS and SANS features

	Flux	Scattered body	Scattering	Resolution	Wavelength	Beam size	Energy
SAXS	~ 10^{11}/cm^2	Electron	Electron density	~ 0.1%	~ 1.5Å	~ 1mm	~ 10keV
SANS	~ 10^{6}/cm^2	Nuclear	Scattering length	~ 10%	~ 10Å	~ 5mm	~ 1meV

adjusted according to the scale of the structure being examined.

2. Research on Structures and Physical Properties in a Molten State

(1) Evaluation of Miscibility in Polyolefin Blends [6]

Neutrons, which were discovered by Chadwick in 1932, have been used for a long time for the magnetic structural analysis of inorganic substances and for determining the positions of hydrogen atoms in organic substances. The advent of the field of polymer science was after the start of the 1970s, and it had its inception with the experimental verification of the theoretical prediction of Flory that "polymer chains in bulk materials are Gauss chains." Neutrons also made a large contribution to the construction of the scaling theory of de Gennes. With the coming of the 1980s, there were a lot of results in the morphological analysis of polymer chains in polymer blend systems, evaluation of the Flory-Huggin's interaction parameter (χ) and research on phase transition in block copolymers.[16]

The conformation of polymer chains in a molten state and molecular interactions effect the subsequent processing and the various properties of molded products, so this information becomes much important for industry. The interaction parameter (χ) is defined when describing the free energy changes of systems acompanied by mixing, and it is an index that shows the strength of the interaction as the product (χN) of the degree of polymerization (N). **Fig. 11** shows schematically the relationship between χN and the conformation of polymer chains.

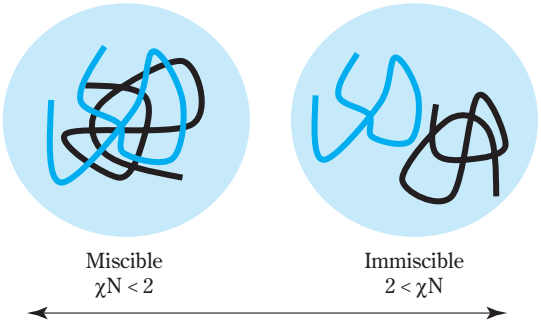

Fig. 11 Conformation of polymer chains in binary blend

SANS can be used in blend systems such as olefin polymers where the physical properties such as the molecular structure, electron density and index of refraction are similar, and it is actually used for the study of miscibility of ethylene-alpha olefin copolymers and isotactic polypropylene (iPP). Quantitative analysis of the interactions taking the molecular structures (amounts and length of short chain branches) of copolymers into consideration is being carried out.[17]

In polyolefin blends without special molecular interactions such as hydrogen bonds, it is assumed that the dispersion force is the dominant interaction that works in the polymer chains, but the mechanism for the miscibility of the polyolefin blends is not well understood. Therefore, we attempted to evaluate the interaction between iPP and atactic propylene-alpha olefin copolymer as a new target for research by using SANS. **Table 4** gives the basic characterization of the samples used in SANS measurements. The quantitative analysis of the interaction parameter (χ) is possible by using 1) deuterated samples and 2) samples for which the copolymer composition is uniform and which have a narrow molecular weight distribution.

Table 4 Characterization of fractionated polymer samples

Sample name	*Mw*	*Mw/Mn*	*Mz*
d-iPP	15,000	1.44	20,000
h-iPP	16,000	1.38	21,200
aPP	35,000	1.34	44,600
a(P/B) (P/B = 80 : 20)[a]	32,600	1.30	42,900
a(P/B) (P/B = 60 : 40)	32,000	1.50	47,000
a(P/B) (P/B = 37 : 63)	37,000	1.34	47,000
a(P/B) (P/B = 13 : 87)	34,000	1.42	44,300
aPB	26,000	1.44	35,100

[a]The ratios between propylene and butene in a(P/B)s are molar ratios

Fig. 12 shows an example of SANS measurement carried out using the small angle neutron scattering device (SANS-U) of the Institute for Solid State Physics at Tokyo University. For analysis of the SANS profile in binary blend systems, the coherent cross section ($d\Sigma/d\Omega$) described by (Eq. 1) is measured as a function of the scattering vector (q), and by reproducing (solid line) the experimental data using the structure factor $S(q)$ expressed by (Eq. 2), χ and the radius of gyration (R_g) can be experimentally estimated.[18]

$$\frac{d\Sigma}{d\Omega} = \left(\frac{b_D}{\upsilon_D} - \frac{b_H}{\upsilon_H}\right)^2 \cdot S(q) \qquad \text{(Eq. 1)}$$

$$S(q)^{-1} = [\upsilon_D N_{w,D} \phi_D P_D(q^2 R_{g,D}^2)]^{-1} + [\upsilon_H N_{w,H} \phi_H P_H(q^2 R_{g,H}^2)]^{-1} - 2\chi_{DH}/\upsilon_0 \qquad \text{(Eq. 2)}$$

Here, b is the scattering length of the monomer, υ the specific molar volume, N_w the weight-averaged molecular weight, ϕ the volume fraction, $P(q^2R_g^2)$ the form factor, q the scattering vector and R_g the radius of gyration. The subscripts D and H indicate deuterium and hydrogen.

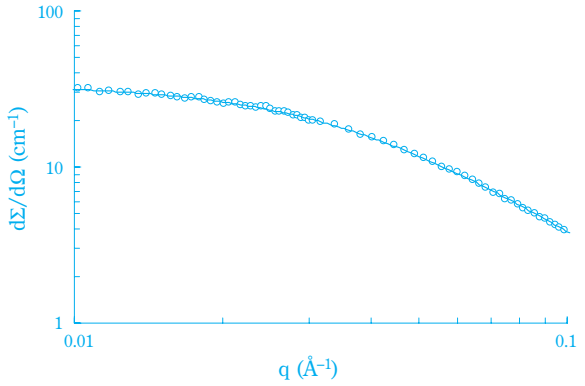

Fig. 12 SANS intensities obtained from d-iPP/a(P/B) (P : B = 60 : 40) blend at 190°C

Fig. 13 shows an example of analysis of the interaction parameter (χ). We can see that the interaction parameter (χ) working in between aPB and iPP has negative values and that it varies dependent on the copolymer composition. These results show that a blend consisting of atactic propylene-butene copolymers and iPP is "miscible blend system" in a molten state.

In addition, from further analysis of the temperature dependence of the interaction parameter (χ), it has become clear in this research that a revision of the theories[19)–21)] proposed in the past paper is necessary to elucidate the interactions working in olefin blends.

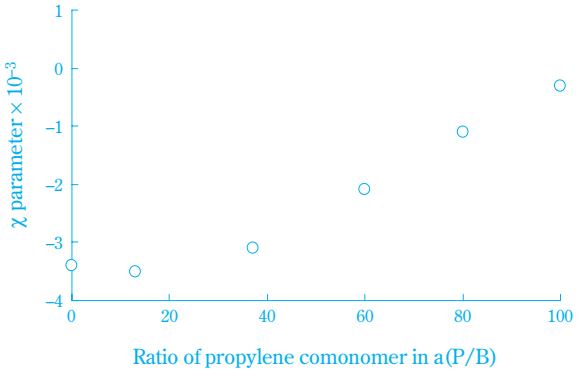

Fig. 13 Flory-Huggins interaction parameter plotted against propylene content in a(P/B)

(2) Observation of the Conformation of Polymer Chains under External Field[7)]

With the progress in device development and testing technology in recent years, SANS has been applied to dynamic structural analysis tasks such as observations of the conformation of polymer chains under shear flow[22)] and *in-situ* observations of living polymerization processes.[23)] **Fig. 14** shows an example of SANS measurements in a steady flow which were carried out in the small-angle neutron scattering spectrometer (SANS-J) at the Japan Atomic Energy Agency. A blend of deuterated high density polyethylene (D-HDPE) and linear low density polyethylene (H-LLDPE) as well as a blend with low density polyethylene (H-LDPE) were used as the samples, and a comparison of SANS images obtained using a small hot shearing machine is shown. At a static state, SANS images indicating that the molecular chains of D-HDPE were of an isotropic morphology were observed for both systems. For a steady flow, SANS images of the D-HDPE/H-LLDPE blend showed elongation of the molecular chains of the HDPE in the direction of the flow. On the other hand, with the D-HDPE/H-LDPE blend, SANS images suggested the flow-induced phase separation of D-HDPE and H-LDPE.

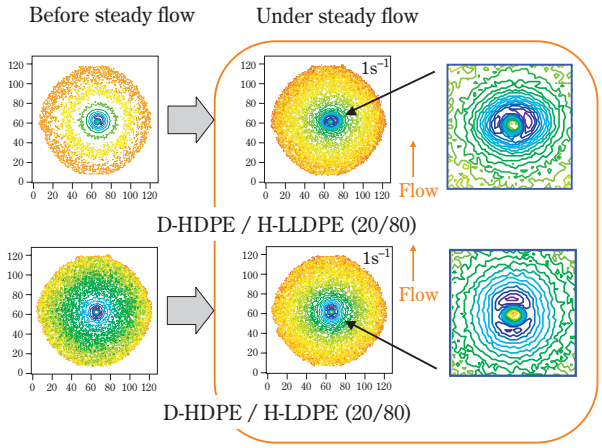

Fig. 14 2D SANS patterns before and under steady flow

SANS is an extremely effective method for evaluating the conformation and miscibility of polymer chains under external force, and while there are still several problems that should be overcome, such as intensity and time resolution, we think it will come into active use in the future as a measurement probe for *in-situ* observations.

3. Evaluation of Solid Structures in Molded Products[8)]

In the field of polymer physics, flow induced crystallization is one of the topics that is being actively debated at present, but it is very complicated because phenomena such as the elongation of the polymer chains and the flow induced phase separation discussed above affect the subsequent crystallization process. In processing stages such as spinning and injection molding, a crystal structure called a "shish kebab structure" is sometimes formed by flow induced crystallization as shown in **Fig. 15**. The crystal structure is named because it has a shape similar to shish kebabs in Turkish cuisine, and consists of plate shaped crystalline structures (kebab structures) and needle shaped crystalline structures (shish structures). It has been widely recognized that the addition of polymers with higher molecular weights accelerates the formation of the shish kebab structure, but the formation mechanism and the role that polymers with other molecular weights play in flow induced crystallization has not been well understood.

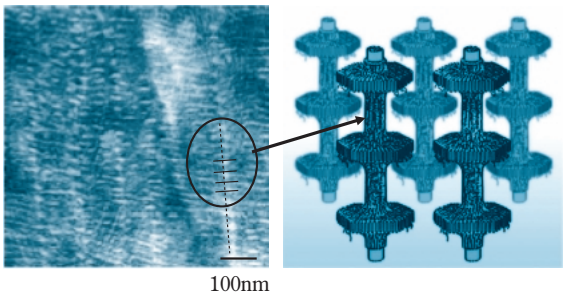

Fig. 15 TEM image of injection molded iPP and schematic illustration of "Shish-Kebab" structure

With the current SANS ability, it is impossible to make *in-situ* observations of flow induced crystallization directly because of the lack of neutron intensity, but through the free use of 1) deuterated labeling and 2) processing technology for small amounts of the sample using small molding machines, we can evaluate only the confirmation of labeled polymers in a sample molded by flow crystallization.

Fig. 16 schematically shows the concept of deuterated labeling that uses SANS when polymers are the target samples. The conformation of D labeled polymers is observed by using SANS in casess where the deuterated polymers (D forms) are substituted for polymers of specific molecular weights in hydrogenated polymers (H forms) or where a small amount of deuterated polymers is added in hydrogenated polymers. There may be an inverse relationship for the ratio by weight of the D form polymer and the H form polymer. We polymerized H form and D form polypropylenes with different molecular weights and prepared a model polymer with a wider distribution of molecular weight and a mixing ratio of numeral 2:4:1 for high, middle and low molecular weights. Finally, we prepared three types of model sample with deuterated labeling in only one component of the whole polymer. **Table 5** gives the basic characteristics of the samples used with SANS. We carried out the SANS measurements by using three types of specimens produced by a special small injection molding machine.[24)]

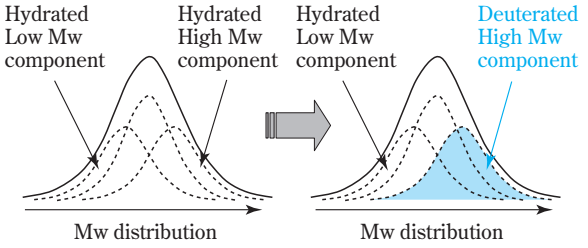

Fig. 16 Schematic illustration for deuterated labeling technique

Table 5 Weight-average molecular mass (*Mw*) and polydispersity (*Mw/Mn*) of the deuterium-labeled fraction and of the blend as a whole

Sample	D-labeled polymer		Blended whole material[a]	
	Mw	*Mw/Mn*	*Mw*	*Mw/Mn*
Low-D	41,000	2.4	467,000	8.3
Mid-D	197,000	3.2	486,000	7.9
High-D	1,781,000	3.1	557,000	8.6

[a]D-labeled polymer contents=13wt%

Fig. 17 shows SANS images obtained from the molded specimens and a comparison with SAX images. All of the SAX images, derived from the differences in the electron density in the samples, showed the same pattern. On the other hand, the SANS images, derived from the D-H contrast, reflected the difference in the molecular weight of the polymers with deuterated labeling, and we obtained scattering patterns with large differences between samples. As a result of detailed

examinations, we confirmed that 1) SANS images derived from shish structures were contained in the direction orthogonal to the direction of flow and 2) low and middle molecular weight components contributed to the formation of shish structures.

These experimental results indicate that the shish formation mechanism is a mechanism in which high molecular weight components play a catalytic role, recruiting middle and low molecular weight polymers adjacent to them into formation of the shish rather than a mechanism that only the high molecular weight components aggregate and forms a shish structure. This finding is extremely important for the elucidation of the nature of the mechanism for forming shish kebab structures.

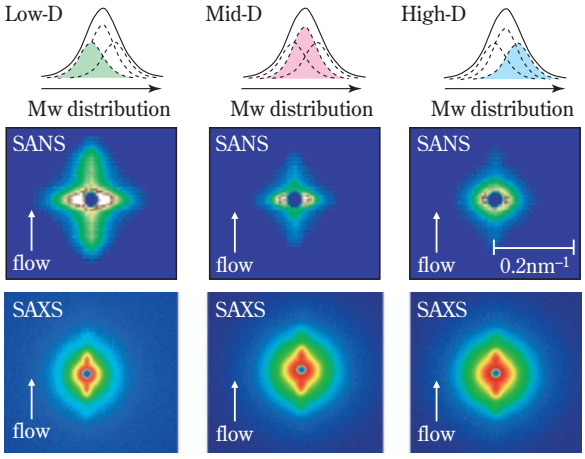

Fig. 17 Comparison of SAXS and SANS patterns obtained from injection molded iPPs with different deuterated Mw component

Conclusion

In this paper, we have described our research on the characterization and analysis of polyolefin' materials using synchrotron radiation as well as neutrons as probes, and described some examples of *in-situ* observation techniques for film drawing behavior and structural evaluation of molded products using the scattering method. Research that uses these quantum beams is extremely effective not only in advanced polymer science but also in the polymer industry, and it will be made use of in the future in the development of newly designed materials and research into product processing. In addition, future research using quantum beams, including infrared and X-ray free electron lasers, is attracting greater expectations as well as the Japan Proton Accelerator Research Complex (J-PARC) with the highest beam power in the world which is planned for construction in Tokai-mura in Ibaragi Prefecture and the construction of the Frontier Soft Matter Development Joint Industry and Academia Beam Line being planned at SPring-8.

Acknowledgements

This research was performed as joint research with the High Energy Accelerator Research Organization, the Japan Atomic Energy Agency and the Institute for Solid State Physics at Tokyo University, and from a general proposal at SPring-8. We would like to express our deep appreciation to Professor Yoshiyuki Amemiya and Assistant Professor Yuya Shinohara of the Graduate School of Frontier Sciences at the University of Tokyo, Professor Yushu Matsushita of the Graduate School of Engineering at Nagoya University, Professor Mitsuhiro Shibayama of the Institute for Solid State Physics at the University of Tokyo and Professor Takeji Hashimoto and Dr. Satoshi Koizumi of the Japan Atomic Energy Agency.

References

1) Y. Ijichi, Y. Saga, T. Fujii, K. Yamamoto, SUMITMO KAGAKU, **1995-II**, 30 (1995).
2) T. Kasahara, N. Yamaguchi, K. Mizunuma, T. Fujii, SUMITMO KAGAKU, **1999-II**, 4 (1999).
3) T. Sakurai, T. Kasahara, N. Yamaguchi, Polymer Applications, **53** (1), 24 (2004).
4) T. Sakurai, Y. Nozue, T. Kasahara, K. Mizunuma, N. Yamaguchi, K. Tashiro, and Y. Amemiya, *Polymer*, **46**, 8846 (2005).
5) Y. Nozue, Y. Shinohara, Y. Ogawa, T. Sakurai, H. Hori, T. Kasahara, N. Yamaguchi, N. Yagi, and Y. Amemiya, *Macromolecules*, **40**, 2036 (2007).
6) Y. Nozue, T. Sakurai, H. Hozumi, T. Kasahara, N. Yamaguchi, M. Shibayama, and Y. Matsushita, *Macromolecules*, **40**, 273 (2007).
7) T. Kasahara, T. Sakurai, T. Fujii, and S. Koizumi, *JAERI-Review*, **2002-028**, 77 (2002).
8) S. Kimata, T. Sakurai, Y. Nozue, T. Kasahara, N. Yamaguchi, T. Karino, M. Shibayama, and J. A. Kornfield, *Science*, **316**, 1014 (2007).
9) H. Oyanagi, "Shinkurotoron hosyako no kiso", Maruzen (1996).
10) K. Ito, Y. Amemiya, Jpn. J. Soc. Synchrotron Radia-

tion Res., **13**, 372 (2000).
11) Sumitomo Chemical Co., Ltd., Jpn. Kokai Tokkyo Koho 2003-207430 (2003).
12) Y. Nozue, Y. Amemiya, Jpn. J. Soc. Synchrotron Radiation Res., **19**, 356 (2006).
13) Sumitomo Chemical Co., Ltd., Applied to Jpn. Tokkyo.
14) J. S. Higgins, and H. C. Benoît, "Polymers and Neutron Scattering", Oxford University Press (1994).
15) Y. Matsushita, "Neutron Beam Analyses and Its Application", Japan Radioisotope Association, Maruzen (1999), p. 94.
16) Y. Matsushita, Chemistry and Chemical Industry, **52** (1), 25 (1999).
17) M. Seki, H. Uchida, Y. Maeda, S. Yamauchi, K. Takagi, Y. Ukai, and Y. Matsushita, *Macromolecules*, **33**, 9712 (2000).
18) P. G. de Gennes, "Scaling Concepts in Polymer Physics", Cornell University Press (1979).
19) F. S. Bates, M. F. Schultz, J. H. Rosedale, and K. Almdal, *Macromolecules*, **25**, 5547 (1992).
20) W. W. Graessley, R. Krishnamoorti, G. C. Reichart, N. P. Balsara, R. J. Butera, L. J. Fetters, and D. J. Lohse, *Macromolecules*, **28**, 1260 (1995).
21) K. F. Freed, and J. Dudowicz, Macromolecules, **31**, 6681 (1998).
22) Y. Takahashi, Y. Ukai, M. Seki, and Y. Matsushita, *Kobunshi Ronbunshu*, **62**, 23 (2005).
23) R. Motokawa, S. Koizumi, T. Hashimoto, T. Nakahira, and M. Yasunaka, *Physica B; Condensed Matter*, **385-386** (1), 780 (2006).
24) J. A. Kornfield, G. Kumaraswamy, and A. M. Issaian, *Ind. Eng. Chem. Res.*, **41**, 6383 (2002).

PROFILE

Takashi SAKURAI
Sumitomo Chemical Co., Ltd.
Petrochemicals Research Laboratory
Research Associate,
PhD in engineering

Tatsuya KASAHARA
Sumitomo Chemical Co., Ltd.
Petrochemicals Research Laboratory
Senior Research Associate
Rabigh Refining & Petrochemical Company

Yoshinobu NOZUE
Sumitomo Chemical Co., Ltd.
Petrochemicals Research Laboratory
Research Associate,
PhD in engineering

Noboru YAMAGUCHI
Sumitomo Chemical Co., Ltd.
Petrochemicals Research Laboratory
Group manager,
Senior Research Associate